PHYSICAL REVIEW B VOLUME 45, NUMBER 12 15 MARCH 1992-II

Quantum bound states in narrow ballistic channels with intersections

Zhen-Li Ji and Karl-Fredrik Berggren
Department of Physics and Measurement Technology, Linköping University, S-581 83 Linköping, Sweden
(Received 1 July 1991)

A quantum-mechanical calculation is made of ballistic transport in intersecting narrow channels of finite length. The two-dimensional (2D) semiconductor structure we study consists of perpendicular channels, one of which connects to two reservoirs of 2D electron gas. These reservoirs serve as emitter and collectors when a potential difference is applied. At a single intersection with infinite leads, there are generally bound states that are well localized to the intersection area. In a structure with finite leads to emitter and collector, such localized states or quantum dots give rise to resonant tunneling. We show that in narrow ballistic channels with few stubs the bound states couple to each other. Therefore, the states at the different intersections combine as split bound states. The splitting is N-fold if there are N intersections. Here we study conductance in structures containing a few crossed-bar or T-shaped junctions and focus on the splitting of the resonance conductance below the first subband threshold. We argue that our results are in qualitative agreement with recent measurements. We also consider the spatial distribution of currents and show that a complicated flow pattern with vortex structures appears at higher energies.

I. INTRODUCTION

Recent progress in nanostructure technology has made possible the fabrication of semiconductor structures whose sizes are smaller than the carrier elastic and inelastic mean free paths.[1,2] Structures of this kind may be achieved by a lateral confinement of the high-mobility two-dimensional (2D) electron gas that resides at the semiconductor interface in a modulation-doped heterostructure like $Al_xGa_{1-x}As/GaAs$. The high speeds and novel electronic properties of these structures make them potential candidates for a new generation of electronic devices. Therefore, it is worth making efforts to clarify and describe the phenomena that occur in such systems. In addition, this type of nanostructure gives rise to a rich physics that deserves to be studied on its own merits. Recently, bound states in laterally constrained two-dimensional systems have received considerable attention.[3–8] Quantum-mechanical calculations show that bound states reside at the intersection of two perpendicular, perfect channels. Although the potential is classically unbound, electrons may thus be trapped at an intersection when their wave-mechanical nature is enhanced; i.e., the crossing channels are made so narrow that transverse quantization and the formation of subbands become characteristic features. This happens when the de Broglie wavelength is comparable to the spatial extension of the structure. On the basis of model calculations, we have recently proposed that bound states at a single intersection may be probed by resonant tunneling.[7,8] A natural question that arises and has been recently studied experimentally and theoretically[9–13] is what happens when there is more than one intersection in the system. This corresponds to the formation of collective states by the coupling of individual states and the interference among the intersections.

The purpose of this paper is to present the results of quantum-mechanical calculations of the conductance for structures with a few intersecting channels. The model we use is a one-electron approximation; i.e., electron interactions and charging effects are not included in this model.[14,15] The reason for using this kind of simplified model is that one needs a general understanding of the one-electron behavior in our type of structures before details associated with charging are considered more explicitly. The actual structures are assumed to be connected to two 2D reservoirs. When a potential difference is applied, electrons flow from one reservoir to the other via the network of quantum channels. We are mainly interested here in the bound states whose energy is less than the threshold energy $E_t=\hbar^2\pi^2/(2m^*w^2)$, i.e., the lowest sublevel associated with a single channel of width w. Below this threshold, the structure in the conductance is simply due to resonant tunneling, and should therefore be easy to recognize and interpret. On the other hand, above threshold, the conductance depends sensitively on geometric variations because of the many possibilities for interference. A distinct quantum transport effect is predicted: The coupling between bound states with energy less than the threshold E_t results in the formation of split-bound states in the systems. The number of split-bound states N corresponds to the number of the intersections in the conducting network. At the same time, the sharp peak in the conductance associated with tunneling through a single intersection is split into N peaks. Such systematic features should emerge clearly in measured data to prove that resonant tunneling indeed takes place. It is interesting to note that there are qualitative similarities with the theoretical predictions for the tunneling conductivity through thin oxide layers grown on metal substrates.[16]

In Sec. II we present the theoretical model. Numerical

results for the conductance are given in Sec. III, and the electron densities associated with the subthreshold resonances are analyzed. The quantum-mechanical current density is elaborated on in Sec. IV. Some concluding remarks are given in Sec. V.

II. THEORETICAL MODEL

Consider a 2D electron gas in, e.g., an $Al_xGa_{1-x}As/GaAs$ modulation-doped heterostructure as referred to above. Assume that a nanopattern is created by introducing also a lateral confinement. In practice, this may be achieved by means of a patterned gate that depletes the electron gas under the gated regions only.

The geometry that we will consider is given in Fig. 1. This particular geometry is chosen because of the recent experiments by Haug *et al.*[9,10] Some similar structures are studied theoretically in Refs. 17 and 18. The recent study by Brum[19] is actually rather similar to the present one. However, methods and the general outlook differ. For example, here considerable emphasis is put on the nature of charge and current distributions.

The pattern in Fig. 1 is oversimplified with respect to its sharp corners. In a real device, these corners would thus be rounded because the conducting regions at the $Al_xGa_{1-x}As/GaAs$ interface derive from smooth electrostatic depletion. For a single channel, for example, sharp corners give rise to "organ pipe" resonances.[20] Such features are unrealistic,[21] but at the same time they are of less of a problem here because we are primarily concerned with the subthreshold behavior that depends on the states trapped at the intersections. Thus we believe that the detailed shape of the potential that confines the electrons to the various channels is not important in determining qualitative aspects of the bound states at the different intersections and how these states couple to each other. Thus we assume a potential that is zero inside the channels and infinite outside, so that the Hamiltonian is just $H=p^2/2m^*$ inside the well; m^* is the electron effective mass. Because of the hard boundaries, the electron wave function vanishes at the edges of the channel. When a weak potential difference is applied at the 2D reservoirs, we have to consider the process by which electrons are injected into the channel connecting the 2D regions and emitted from it. In doing so, we use Kirczenow's[20] analogous ballistic model for a single short channel in between two 2D reservoirs. In the region containing the constrictions, the wave function may be expanded in a complete set of solutions of the Schrödinger equation in each of the 13 rectangular regions shown in Fig. 1. Consider a free electron with wave vector $\mathbf{k}=(\kappa,k)$ incident on the channel opening from the left. The corresponding wave function is[8,20]

$$\Psi_L(x,y)=e^{i\kappa+iky}+\int_{-\infty}^{\infty} dk' A_L(k')e^{-i\kappa' x+ik'y} , \quad (1)$$

where the last term accounts for backscattering. For the electron emitted into the reservoir on the right-hand side, one has

$$\Psi_R(x,y)=\int_{-\infty}^{\infty} dk' A_R(k')e^{i\kappa' x+ik'y} . \quad (2)$$

Within the horizontal channels ($I=1,5,9,13$ in Fig. 1), the expansions are of type

$$\Psi_I(x,y)=\sum_n (B_{I,n}e^{q_n x}+C_{I,n}e^{-q_n x}) \times \sin\left[\frac{n\pi}{w}\left[y+w/2\right]\right] , \quad (3)$$

where w is the width of the channels and n refers to sublevels. The expansion is similar in the remaining regions.[8] The quantity q_n is determined by the energy E of the electron injected from the emitter to the left, and can be either real or imaginary depending on whether E is below or above sublevel E_n. The wave function is expanded in similar ways in the remaining channel areas. Matching amplitudes and derivatives at every boundary, we find a system of linear equations for the expansion coefficients $B_{I,n}$ and $C_{I,n}$. We solve this system numerically, and use the solution to calculate the conductance at zero temperature as an expectation value over the operator for the quantum-mechanical current. Details of this procedure are found in Refs. 3, 8, and 20. The current is also discussed in Sec. IV.

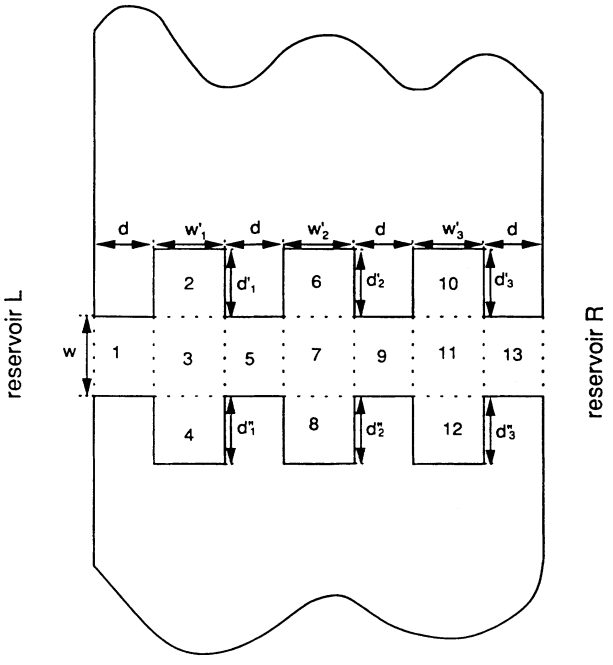

FIG. 1. Schematic representation of the "network" connecting left (L) and right (R) reservoirs of 2D electrons with equal Fermi energy. When the potential difference is applied, electrons flow from L to R. The regions 1–13 are used in the expansion of wave functions that are to be matched across the boundaries represented by the dashed lines.

III. CONDUCTANCE AND RESONANT-TUNNELING STATES

In the following, we will assume an effective mass $m^*=0.067m_0$, which is appropriate for the

$Al_xGa_{1-x}As/GaAs$ interface. In Figs. 2(a)–2(c), the calculated conductance G is given for three different structures, namely a single, a double, and a triple cross. We have chosen to plot G as a function of the Fermi energy, keeping the dimensions of the structures constant. The change in energy corresponds to a variation of the density of the 2D gas in the emitter and collector regions. From a practical point of view, one would rather vary the dimensions of the structure uniformely by means of, e.g., an applied gate voltage. In both cases, however, the Fermi energy is made to sweep through the different energy levels. Qualitatively, the physics should therefore be the same in the two cases.

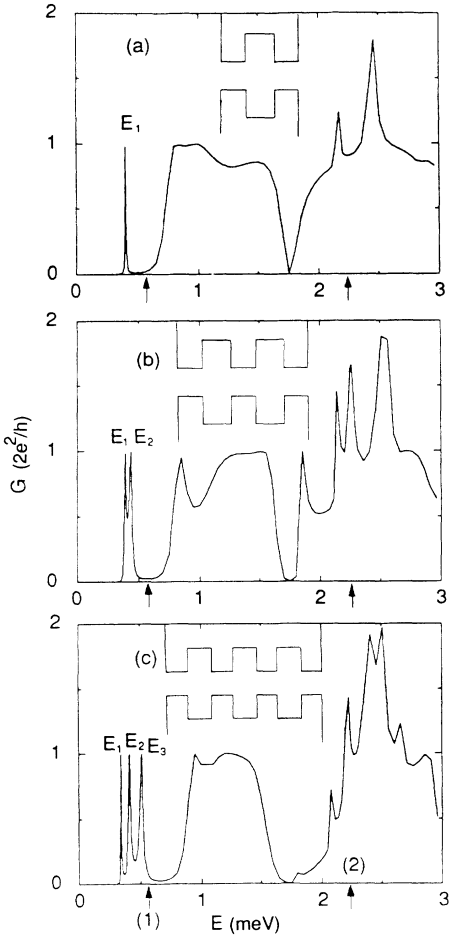

FIG. 2. Calculated conductance at zero temperature as a function of the Fermi energy E. The width of the channel connecting the $2D$ regions and the distance among the stubs are kept constant, $w=100$ nm and $d=20$ nm. Cases (a) and (b) correspond to removing stubs in the constriction of Fig. 1. For (a) we remove the two outermost stubs by choosing $w_1'=w_3'=30$ nm, $w_2'=100$ nm, $d_1'=d_1''=d_3'=1$ nm, $d_2'+d_2''=50$ nm. For (b) we remove the middle stub with the choice $w_1'=w_3'=100$ nm, $w_2'=30$ nm, $d_1'=d_1''=d_3'=d_3''=50$ nm, $d_2'=d_2''=1$ nm. Case (c) refers to the full structure with three stubs with $w_i'=100$ nm, $d_i'=d_i''=50$ nm, $i=1$, 2, and 3. The positions for the two lowest sublevels are indicated by arrows labeled (1) and (2). E_1, E_2, and E_3 denote energies at which resonant tunneling via states resembling quantum dots takes place.

We first consider the case of a single cross. This case is obtained by letting $d_1'=d_1''=d_3'=d_3''=0$; i.e., the outermost stubs are removed. In practice, however, one would have to chose a small value (~ 1 nm) instead of zero to attain numerical stability. Otherwise, the difference between the two choices for the d's is, of course, insignificant. Figure 2(a) clearly shows a peak in the conductance G below the lowest subband threshold $E_t=\hbar^2\pi^2/(2m^*w^2)$. This peak is to be expected, since it corresponds to tunneling through the state residing at the center of the cross, i.e., the localized bound state in the case of two infinite, crossing channels. The resonance peak is sharp and acquires its maximum value $2e^2/h$ because the corresponding state is well localized to the intersection itself, and is well separated from the first subband. Actually, we may view this state as a quantum dot, and the tunneling as occurring via such a dot.

Although our main concern is the conductance near threshold, we will briefly comment on what happens at higher energies. The conductance in Fig. 2(a) for energies above E_t is related to traveling-wave states associated with the subbands. For a single channel, one would ideally have quantized plateaus corresponding to the different subbands.[22,23] A single intersection as in Fig. 2(a) modifies this picture drastically. Because of destructive quantum-mechanical interference, the conductance is even seen to vanish at some energy below the second subband. Also, the conductance for energies in the second subband deviates strongly from the ideal quantization. Close to the second subband threshold, we note two other pronounced peaks. The lower one corresponds to the next lowest bound state in two intersecting infinite channels, and the second to a resonance associated with the finite extension of the stubs.[8] These peaks do not attain ideal quantization in units of $2e^2/h$ because they are immersed in or interact with a subband continuum. This situation is thus different than for the lowest resonance, which is well separated from the subbands.

If we now consider the case of a double cross as in Fig. 2(b), the tunneling below threshold could be thought of as a tunneling via two quantum dots, one at each intersection. If the corresponding states are spatially close enough to interact weakly, the resonance should split into two peaks. If we assume that the interaction energy between two dots is V, the split levels $E_{1,2}$ and eigenvectors $\mathbf{C}_{1,2}$ are given by

$$E_{1,2}=E_0\pm V\ ,\qquad \mathbf{C}_{1,2}=(1,\mp 1)/\sqrt{2}\ , \tag{4}$$

where E_0 is the single-site energy and the elements of the vector refer to single quantum-dot wave functions localized to the different intersections. As is to be expected, we obtain a bonding and an antibonding state with energies E_1 and E_2, respectively. As for the single cross, we find that the conductance may vanish at higher energies due to destructive interference and that the two peaks close the second subband threshold both split into two new peaks.

Let us now consider the case of a triple cross. It is interesting to compare this case with calculations of the

tunneling current through thin metal-oxide layers grown on the metal substrate.[16] Scanning-tunneling-microscopy (STM) measurements for NiO on Ni(100) have shown three distinct peaks in the STM spectra that may be explained as resonant tunneling through weakly coupled oxide states in the three layers. The tunneling is in this case conveniently described by means of a Kronig-Penney model or δ functions representing the different layers. Although our system is a very different one, the physics is quite the same. In our case, we should then expect a resonance structure below the lowest subband threshold that mirrors three weakly interacting quantum dots. If the interaction V is limited to nearest neighbors only, the three quantum dots combine as

$$\begin{aligned} &E_{1,3}=E_0\pm\sqrt{2}V\ , \\ &\mathbf{C}_{1,3}=(1,\mp\sqrt{2},1)/2\ , \\ &E_2=E_0\ , \\ &\mathbf{C}_2=(1,0,-1)/\sqrt{2}\ . \end{aligned} \tag{5}$$

States of this kind are also discussed in Ref. 16. Figure 2(c), which is based on the exact calculations outlined in Sec. II, shows clearly the three distinct resonance peaks in accordance with our simple qualitative arguments about coupled quantum dots. We also notice that the conductance reaches it maximum value $2e^2/h$ at the resonances. This happens when the separate quantum-dot wave functions are well localized to an intersection and well separated from the first subband. Above the threshold energy E_t, we find the same behavior as above, but the two peaks of Fig. 2(a) are now split into three peaks each. Since we are mainly concerned with the behavior close to threshold, these peaks are, however, not well resolved numerically.

In summary, we conclude that the resonance peak below the lowest subband threshold is split into N peaks if there are N intersections or crosses in the structure connecting the two 2D reservoirs. The transport may be viewed as tunneling or hopping via coupled quantum dots at the different intersections. If the coupling is weak, the splitting is small, and vice versa. This is shown explicitly in Figs. 3(a) and 3(b), which show the calculated conductance for two crosses with different degrees of coupling. If the states associated with the resonant tunneling are well localized to the intersections, i.e., the stubs are sufficiently extended, the resonance peaks are well below the first subband threshold and the conductance is found to equal $2e^2/h$ at resonance.

Finally, we consider the T structures studied experimentally by Haug, Lee, and Hong[9] that correspond to removing the upper stubs in Fig. 1 by choosing $d_i'=0$ (or any small value in accordance with the remarks above). In a single-T structure with infinitely long leads, there is one bound state below E_t as for the crossed bars.[7] In fact, this is the only bound state in this case. Coupling the T's in series in between the emitter and collector regions, we should thus recover the split resonant tunneling as above. Figure 4 shows the expected splitting for the case of a three-finger structure. Figure 5 shows the electron densities associated with the resonance states. Since the states are strongly concentrated to the intersections, these densities are essentially the same as for the bound states in structures with infinite leads. Figure 5(a) thus displays the density for a single T. Figures 5(b)–5(d) show how states of this kind combine to form the three split resonance states at energies E_1, E_2, and E_3 in rough agreement with Eq. (5). Figure 4 is based on a somewhat course mesh in energy in order to save computer time. Although the numerical resolution is reduced in this way, the figure still shows the principal feature we want to emphasize here, namely, the three-peak structure at threshold. However, we have not cared to locate exactly the

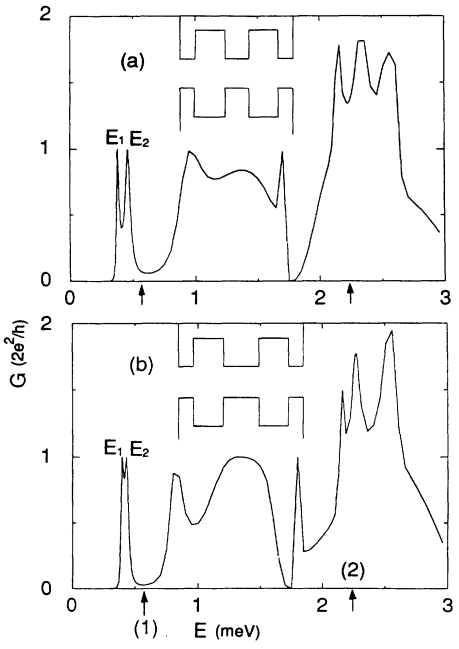

FIG. 3. Zero-temperature conductance of the constriction vs Fermi energy E. Here $w=w_1'=w_3'=100$ nm, $d=10$ nm, $d_1'=d_1''=d_3'=d_3''=50$ nm, $d_2'=d_2''=1$ nm for all cases. (a) and (b) refer to $w_2'=20$ and 60 nm, respectively; i.e., the interaction between the quantum dots is made weaker by increasing the separation of the intersections. General notations are the same as in Fig. 2.

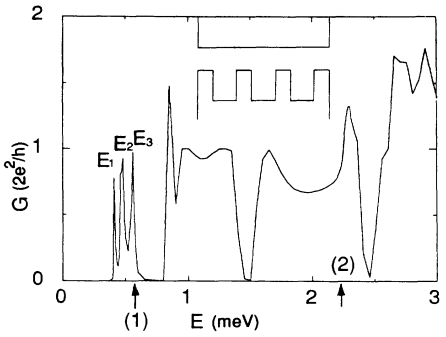

FIG. 4. The conductance G at zero temperature vs Fermi energy E for an unsymmetrical constriction consisting of three coupled T's. Here $w=w_i'=100$ nm, $d=20$ nm, $d_i'=1$ nm, $d_i''=120$ n, $i=1$, 2, and 3. General notations are the same as in Fig. 2.

maximum values at the peaks. When comparing with measurements, this is also of less concern, because it is hard to go beyond qualitative arguments for the following reasons. Conductance measurements are obtained by varying the applied gate voltage that determines the electrostatic depletion regions and hence the structure. Both the Fermi energy and the geometric structure change. In addition, for real structures, the relation between gate voltage and the geometry is not well defined. This precludes any detailed comparison with experimental result. Rather, we should look for principal features.

Our calculations have shown that interactions between the different intersections cause a splitting of the resonance below the first subband threshold. This splitting is found here to be qualitatively the same for coupled crosses and T structures. In fact, it should be a general feature of any geometry containing N interacting intersections that there is N-fold splitting. Such an imprint should be easy to distinguish in measured data. The systematic correlation between the number of peaks near threshold and the number of fingers in the experimental structure of Haug *et al.*[9,10] suggests that these peaks are indeed due to resonant tunneling via coupled quantum dots. The observed conductance is, however, less than the ideal theoretical value for ballistic transport. Obviously, the presence of imperfections in a real device should generally have such a consequence. We should also recall that our calculations are based on a very simplified model potential. As shown in Fig. 5, the charge accumulates in certain regions of the structure. Hence the electrostatic potential should vary, and the wave functions we use should be considerably modified if such variations in the potential are treated self-consistently. This will tend to reduce ballistic transport, as discussed already by Escapa and García.[24] It is, however, beyond the scope of the present model study to include self-consistency.

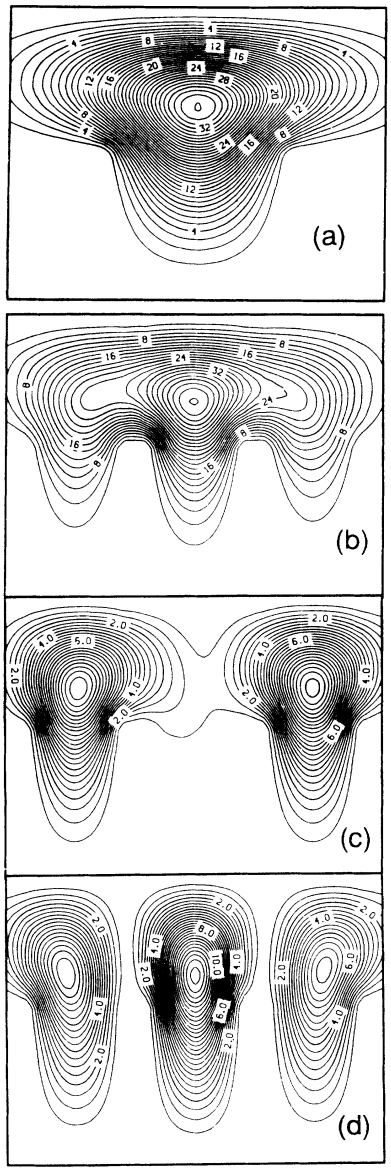

FIG. 5. Electron densities for the resonance states below the subband threshold E_t in the T-shaped structures of Ref. 9. Case (a) shows the density for a single T. One notes the high degree of localization that makes the state akin to a quantum dot. Cases (b)–(d) show how states essentially consisting of coupled quantum dots are formed in rough agreement with Eq. (5).

The measured data also reveal structure above threshold that does not agree with our computed results. Also, the observed conductance does not really vanish for any of the gate voltages applied. Again, we believe this is related to imperfections. Transport above subband thresholds takes place by means of traveling waves that interfere in a delicate way. Perfect interference of this kind is the cause of the zero conductance that may appear above threshold, according to our model calculations. We would like to argue that imperfections easily disturb such interference. Above threshold, the observed data would therefore be contaminated with noise. On the other hand, below threshold, the structure appears much more robust, since we are dealing with localized states that are linearly combined in a simple way. Our discussion about the effect of imperfections is obviously speculative. It would therefore be illuminating to perform realistic simulations on nanostructures, allowing for a large number of imperfections. The present method is, however, not well suited for such a study.

IV. SPATIAL VARIATIONS OF CURRENTS

The transport properties discussed above appear to be uniquely quantum mechanical. Thus the resonant tunneling and the off state due to interference are phenomena that are distinctly nonclassical. One may then ask the question of whether the corresponding currents and their spatial variations will also show unexpected features. This aspect seems to have achieved less attention. Actually, the classical calculation by Beenakker and van Houten[25] claims that many of the anomalies in multilead microstructures, such as the quenching of the Hall resistance, are surprisingly well explained by treating an electron as a classical billiard ball.[26] In the billiard model, the transmission probabilities are obtained by counting the number of classical electron trajectories in the specific sample geometries, neglecting the discreteness of a transverse momentum and the interference among Feynman

trajectories. Although certain features of small quantum structures may be understood by means of "pinball" models,[27] we will find below that the wave-mechanical interference gives rise to a vortex flow that is hardly explained in such terms.

In a situation with ballistic transport, a one-electron description of the flow of electrons is relevant. For an electron with initial wave vector $\mathbf{k}$, the quantum-mechanical probability current density at position (x,y) is

$$\mathbf{i}_{\mathbf{k}}(x,y)=\frac{1}{2m^*}(\Psi\mathbf{p}\Psi^*+\Psi^*\mathbf{p}\Psi)\ , \tag{6}$$

where $\mathbf{p}$ is the momentum operator and Ψ is any of the wave functions as defined above for the different regions of the structure. The total probability current density $\mathbf{I}(x,y)$ is obtained by integrating over all incoming electrons:

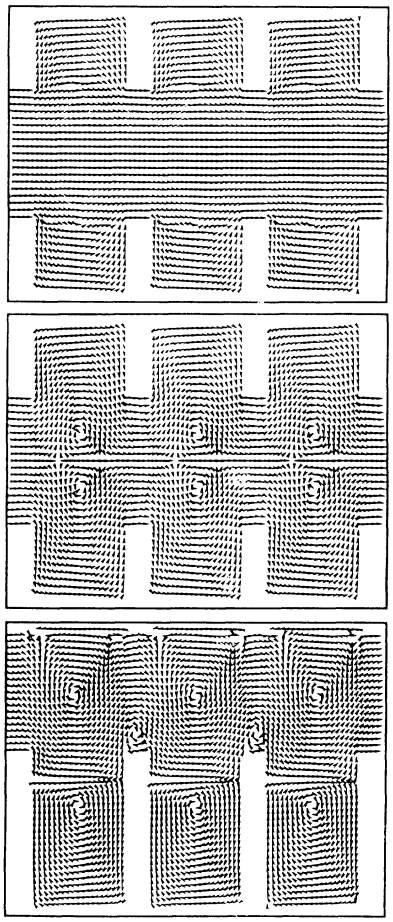

FIG. 6. Plots of the quantum-mechanical probability current density. Case (a) shows the distribution of current in a triple-cross structure at resonance [energy E_1 in Fig. 2(c)]. Case (b) refers to the same structure as (a) but with a higher energy, $E=1.6$ meV. At this energy the conductance is small because of quantum-mechanical interference. Case (c) shows the probability current density in the triple T structure of Fig. 4 when $E=1.4$ meV. Also, in this case, G is small because of interference.

$$\mathbf{I}(x,y)=2\int_{K_0}^{k_F}k\,dk\int_{-\pi/2}^{\pi/2}d\phi\,\mathbf{i}_{\mathbf{k}}(x,y)/(2\pi)^2\ , \tag{7}$$

where $\mathbf{k}=k(\cos\phi,\sin\phi)$ and the factor of 2 derives from spin. Let E_F be the Fermi energy and eV the drop in potential energy across the constriction. Because of the Pauli principle, only electrons in the energy range (E_F-eV,E_F) are allowed to flow from the emitter to the collector. Then $k_F=(2m^*E_F)^{1/2}/\hbar$ and $k_0=[2m^*(E_F-eV)]^{1/2}/\hbar$ in Eq. (7). If the applied voltage difference is infinitesimal, we obtain

$$\mathbf{I}(x,y)=\frac{2m^*}{h^2}eV\int_{-\pi/2}^{\pi/2}d\phi\,\mathbf{i}_{\mathbf{k}}(x,y)\ , \tag{8}$$

where the magnitude of $\mathbf{k}$ equals k_F. If this expression is integrated over coordinate (y), the expression for the conductance given in Ref. 8 is easily recovered. Figure 6 shows the probability current density at two situations for which wave-mechanical aspects should be essential, namely at resonance and at strong interference in the region near zero conductance. The flow of electrons is quite smooth at resonance, which seems consistent with the concept of resonant tunneling. In the second case, the flow develops an unexpected and complex pattern with vortices. With increasing energy, this pattern becomes increasingly complex. Cases appear when small changes in the initial conditions, i.e., Fermi energy or the dimensions of the structure, induce large changes in the flow pattern. In this sense, the behavior of the current distribution reminds one of turbulence. Actually, the behavior is so complex that it ideally renders itself to animation. A detailed study of transport through a single cross is given in Refs. 28 and 29.

V. BRIEF SUMMARY

In conclusion, we have studied theoretically the ballistic transport in some nanostructures at zero temperature. We have shown that the bound states below the first sublevel split into several bound states due to the coupling of bound states in narrow ballistic channels with a few intersections. The number of the split bound states is correlated with the number of the intersections of the 2D semiconductor structure. Experimentally, such features should be easy to identify, provided that resonant tunneling can be achieved in practice. We propose that the measurements by Haug *et al.*[9,10] may be interpreted in these terms. We have also shown that the spatial distribution of currents is nonclassical and may display a very complex pattern in which vortices emerge clearly. Extension of this work to include finite temperatures and electric fields and to more realistic modeling of the confining potential, including scattering from potential fluctuations and other imperfections, appears interesting but remains to be done.

ACKNOWLEDGMENTS

This work was partially supported by the Swedish Natural Science Research Council and the Swedish National Board for Technical Development. Informative discussions with C. Besev at the National Supercomputer Centre at Linköping University are gratefully acknowledged.

[1]For a general overview of the physics of ultrasmall structures, see *Nanostructure Physics and Fabrication,* edited by M. A. Reed and W. P. Kirk (Academic, New York, 1989).

[2]*Nanostructures: Fabrication and Physics,* edited by S. D. Berger, H. G. Craighead, D. Kern, T. P. Smith III, and S. D. Berger, MRS Symposia Proceedings No. EA-26 (Materials Research Society, Pittsburgh, 1990).

[3]R. L. Schult, D. G. Ravenhall, and H. W. Wyld, Phys. Rev. B **39**, 5476 (1989).

[4]F. M. Peeters, Superlatt. Microstruct. **6**, 217 (1989).

[5]J. L. D'Amato, H. M. Pastawski, and J. F. Weisz, Phys. Rev. B **39**, 3554 (1989).

[6]F. Sols and M. Macucci, Phys. Rev. B **41**, 11 887 (1990).

[7]K.-F. Berggren and Zhen-Li Ji, Superlatt. Microstruct. **8**, 59 (1990).

[8]K.-F. Berggren and Zhen-Li Ji, Phys. Rev. B **43**, 4760 (1991).

[9]R. J. Haug, K. Y. Lee, and J. M. Hong, in *Nanostructures: Fabrication and Physics* (Ref. 2), p. 29.

[10]R. J. Haug, K. Y. Lee, T. P. Smith III, and J. M. Hong, in *Proceedings of the 20th International Conference on the Physics of Semiconductors,* edited by J. Joannopoulos (World Scientific, London, 1990), p. 2443.

[11]H. U. Baranger, Phys. Rev. B **42**, 11 479 (1990).

[12]R. L. Schult, H. W. Wyld, and D. G. Ravenhall, Phys. Rev. B **41**, 12 760 (1990).

[13]J. Rundquist, Zhen-li Ji, and K.-F. Berggen, in *Nanostructures: Fabrication and Physics* (Ref. 2), p. 87.

[14]U. Meirav, M. A. Kastner, and S. J. Wind, Phys. Rev. Lett. **65**, 771 (1990), and references cited therein.

[15]C. W. J. Beenakker, Phys. Rev. B **44**, 1646 (1991).

[16]R. García, J. J. Sáenz, and N. García, Phys. Rev. B **33**, 4439 (1986).

[17]L. P. Kouwenhoven, F. W. J. Hekking, B. J. van Wees, C. J. P. M. Harmans, C. E. Timmering, and C. T. Foxon, Phys. Rev. Lett. **65**, 361 (1990).

[18]F. M. de Aguiar and D. A. Wharam, Phys. Rev. B **43**, 9984 (1991).

[19]J. A. Brum, Phys. Rev. B **43**, 12 082 (1991).

[20]G. Kirczenow, Phys. Rev. B **39**, 10 452 (1989).

[21]A. Szafer and A. D. Stone, Phys. Rev. Lett. **62**, 300 (1989).

[22]B. L. van Wees, H. van Houten, C. W. J. Beenakker, J. G. Williamson, L. P. Kouwenhoven, D. van der Marel, and C. T. Foxon, Phys. Rev. Lett. **60**, 848 (1988).

[23]D. A. Wharam, T. J. Thornton, R. Newbury, M. Pepper, H. Ahmed, J. E. F. Frost, D. G. Hasko, D. C. Peacock, D. A. Ritchie, and G. A. C. Jones, J. Phys. C **21**, L209 (1988).

[24]L. Escapa and N. García, Appl. Phys. Lett. **56**, 901 (1990).

[25]C. W. J. Beenakker and H. van Houten, Phys. Rev. Lett. **63**, 1857 (1989); *Electronic Properties of Multilayers and Low-Dimensional Semiconductor Structures,* edited by J. M. Chamberlain, L. Eaves, and J. C. Potal (Plenum, London, 1990).

[26]M. L. Roukes, A. Scherer, and B. P. Van der Gaag, Phys. Rev. Lett. **64**, 1154 (1990).

[27]S. Washburn, Nature **353**, 119 (1991).

[28]K. F. Berggren, C. Besev, and Zhen-Li Ji, Phys. Scr. (to be published).

[29]K. F. Berggren, C. Besev, and Zhen-Li Ji, *Proceedings of the International Workshop on Quantum-Effect Physics, Electronics and Applications, Luxor, Egypt, 1992* (Institute of Physics, Bristol, in press).